Bioresource Technology 380 (2023) 129068

Contents lists available at ScienceDirect

Bioresource Technology

journal homepage: www.elsevier.com/locate/biortech

Characterizing isoprene production in cyanobacteria – Insights into the effects of light, temperature, and isoprene on *Synechocystis* sp. PCC 6803

João S. Rodrigues [a], László Kovács [b], Martin Lukeš [c], Rune Höper [d], Ralf Steuer [d], Jan Červený [e], Pia Lindberg [a], Tomáš Zavřel [e,*]

[a] *Department of Chemistry - Ångström, Uppsala University, Sweden*
[b] *Institute of Biophysics, Biological Research Centre, Szeged, Hungary*
[c] *Institute of Microbiology, The Czech Academy of Sciences, Třeboň, Czech Republic*
[d] *Institute for Biology, Theoretical Biology (ITB), Humboldt-University of Berlin, Berlin, Germany*
[e] *Department of Adaptive Biotechnologies, Global Change Research Institute of the Czech Academy of Sciences, Brno, Czech Republic*

HIGHLIGHTS

- Isoprene producing *Synechocystis* sp. PCC 6803, and two control strains were tested.
- Violet light and increased temperature of 35–40 °C favored isoprene production.
- The presence of isoprene allowed for long-term surviving of *Synechocystis* at 40 °C.
- The presence of isoprene increased membrane fluidity in *Synechocystis*.
- Thermotolerance improvement by isoprene can be transferred between organisms.

GRAPHICAL ABSTRACT

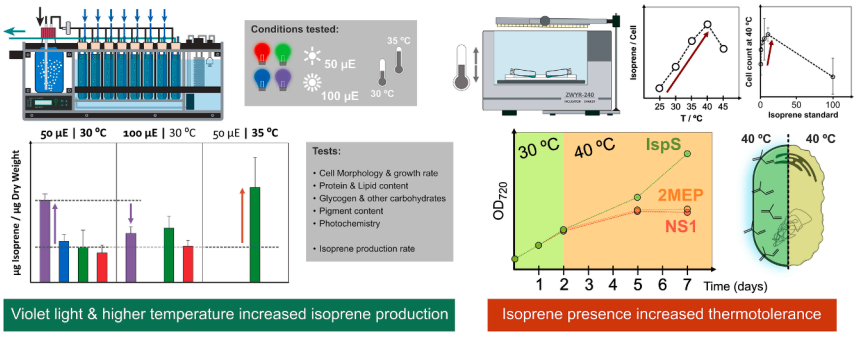

ARTICLE INFO

Keywords:
Biofuels
Cultivation conditions
Optimization
Thermotolerance
Flux Balance Analysis

ABSTRACT

Engineering cyanobacteria for the production of isoprene and other terpenoids has gained increasing attention in the field of biotechnology. Several studies have addressed optimization of isoprene synthesis in cyanobacteria via enzyme and pathway engineering. However, only little attention has been paid to the optimization of cultivation conditions. In this study, an isoprene-producing strain of *Synechocystis* sp. PCC 6803 and two control strains were grown under a variety of cultivation conditions. Isoprene production, as quantified by modified membrane inlet mass spectrometer (MIMS) and interpreted using Flux Balance Analysis (FBA), increased under violet light and at elevated temperature. Increase of thermotolerance in the isoprene producer was attributed to the physical presence of isoprene, similar to plants. The results demonstrate a beneficial effect of isoprene on cell survival at higher temperatures. This increased thermotolerance opens new possibilities for sustainable bio-production of isoprene and other products.

* Corresponding author at: Department of Adaptive Biotechnologies, Global Change Research Institute of the Czech Academy of Sciences, Brno, Czech Republic.
E-mail address: zavrel.t@czechglobe.cz (T. Zavřel).

https://doi.org/10.1016/j.biortech.2023.129068
Received 24 February 2023; Received in revised form 3 April 2023; Accepted 16 April 2023
Available online 19 April 2023

1. Introduction

Isoprene is a volatile five-carbon-atom terpene, the smallest member of the vast family of terpenes and terpenoids. It is generated in certain plants in response to heat stress and globally, isoprene production by plants has been estimated to exceed 500 Tg C yr^{-1} (Guenther et al., 1995). When produced in leaves, isoprene provides the plant with protection against thermal and oxidative stress (Sharkey & Yeh, 2001; Singsaas et al., 1997; Pollastri et al., 2021). Besides its role as antioxidant, acting as scavenger of reactive oxygen species (ROS), it may also have a complex role in the plant response to heat stress (Pollastri et al., 2021; Zuo et al., 2019). Furthermore, isoprene confers increased thermostability to the thylakoid membranes in plants (Velikova et al., 2011).

Apart from its biological function in plants, isoprene has industrial use as a precursor for chemical production processes such as synthetic rubber manufacturing. To date, isoprene is derived exclusively from petrochemical sources and it is used on a scale of more than 750 000 tons annually (Whited, 2010). The sizeable demand for isoprene combined with its impact on the global carbon footprint has led isoprene to be identified as a potential target for sustainable biotechnological production. Due to its volatile nature, it can be produced in cell cultures and harvested from the gas phase, simplifying downstream processing (Whited, 2010; Lindberg et al., 2010). While some microorganisms, such as *Bacillus subtilis* (Kuzma et al., 1995; Wagner et al., 2000), can produce isoprene naturally, most efforts at sustainable bioproduction of isoprene have focused on engineered strains.

Photosynthetic production of isoprene, using cyanobacteria as host cells, would be beneficial as it allows for direct conversion of CO_2 into the desired product in a single cell, with energy provided by solar light. Cyanobacteria are capable of producing terpenoids via the methylerythritol 4-phosphate (MEP) pathway (Rohmer, 1999), and heterologous production of isoprene in cyanobacterium model strains such as *Synechocystis* sp. PCC 6803 (hereafter *Synechocystis*) has been demonstrated (Rodrigues & Lindberg, 2021; Chaves & Melis, 2018). Heterologous isoprene production in cyanobacteria may be expected to have effects on the cell similar to those in plants, but this has so far not been extensively investigated.

The production of terpenoids in cyanobacteria is likely subjected to tight regulation, and linked to regulation of photosynthesis and central metabolism, as has been demonstrated for the MEP pathway in plant chloroplasts (Banerjee & Sharkey, 2014). To develop cyanobacteria as a chassis for sustainable isoprene bio-production, it is first necessary to understand resource allocation shifts in the isoprene producers, including alterations in growth, photosynthetic efficiency and energy and carbon partitioning. As suggested recently (Klaus et al., 2022), it is paramount to evaluate how the isoprene producing cells will respond to specific growth conditions, such as different light spectrum or intensity, that may affect the regulation of terpene biosynthesis. In plants, flux through the MEP pathway to isoprene synthesis is closely linked to the availability of reducing power in (NADPH, reduced ferredoxin), as well as to the levels of ATP (Banerjee & Sharkey, 2014). In a recent study, mixotrophic ^{13}C-metabolic flux analysis revealed that the isoprene producing *Synechocystis* exhibited a higher flux through the MEP pathway and TCA cycle, while flux through CBB cycle towards glycogen formation were reduced, likely also as a consequence of altered ATP and NADPH availability (Nirati et al., 2022). Furthermore, it is of interest to investigate if isoprene has an effect on thermotolerance of cyanobacteria, as observed in plants (Pollastri et al., 2021; Velikova et al., 2011), as this may open new avenues for using cyanobacteria as a model to study responses to heat stress in a plant-like system.

To address these emerging and still unresolved issues, three engineered *Synechocystis* strains were compared in this study: an isoprene-producing strain, which expresses the isoprene synthase from *Eucalyptus globulus* together with two enzymes from the MEP pathway; a control strain, only overexpressing the two MEP enzymes; and another control strain, only overexpressing the antibiotic resistance. All strains were subjected to extensive quantitative evaluation under a range of cultivation light wavelengths, light intensities and temperatures, and shifts in isoprene production and resource allocation strategies were quantified. This allowed to identify isoprene production bottlenecks. In addition, the effect of isoprene on cyanobacterial survival at elevated temperatures was investigated.

The results can lead a way of thermotolerance improvement in biotechnology - an issue expectedly emerging in the context of global warming. The identified key factors affecting isoprene phototrophic production (increased temperature, violet light), together with the finding that isoprene production is not coupled with growth, are expected to guide further optimization strategies for strain engineering, as well as improved cultivation setups towards sustainable isoprene bioproduction.

2. Material and methods:

2.1. Strains generation and cultivation

2.1.1. Plasmid assembly

The isoprene-producing strain (denoted as IspS here) was generated in a previous study (Rana et al., 2022). This strain was designed for expression of codon-optimized versions of 1-deoxy-D-xylulose 5-phosphate synthase (DXS) from *Coleus forskohlii*, the native isopentenyl diphosphate isomerase (IDI) and the isoprene synthase (IspS) from *Eucalyptus globulus* (EgIspS), whose genes were integrated in the *slr0168* locus of the cyanobacterial chromosome (Kunert et al., 2000).

In order to generate a control strain that overexpressed DXS and IDI but lacked the EgIspS expression, the CfDxs-SynIdi operon alone was amplified by PCR from the p6EgIspS plasmid (Englund et al., 2018), and cloned it into the pEERM3 plasmid using the EcoRI and XbaI restriction enzymes. The resulting plasmid was designated as pEERM3_2MEP.

2.1.2. Strains generation

Control strains were transformed via natural transformation as described previously (Heidorn et al., 2011), for chromosomal integration of the synthetic devices in *slr0168* neutral site (Kunert et al., 2000) together with a kanamycin resistance cassette. The resulting strains were named “2MEP” (integrating pEERM3_2MEP) and “NS1” (integrating kanamycin cassette alone within pEERM3). For further details on strains generation, see supplementary material.

Colonies of the 2MEP and NS1 strains were cultured on BG-11 agar plates supplemented with 50 μg mL^{-1} of kanamycin, and positive transformants were confirmed by colony PCR. The integration of the constructs into the *slr0168* locus was achieved by cultivation of the strains over several rounds in BG-11 (Stanier et al., 1971) liquid medium supplemented with 50 μg mL^{-1} kanamycin. Genomic DNA was extracted (GeneJET Genomic DNA purification kit, Thermo Fischer Scientific, USA) and used as a template for PCR analysis to confirm full segregation of the strains.

2.1.3. Strains cultivation

The inoculum strains were cultivated in Erlenmeyer flasks in BG-11 cultivation medium supplemented with 50 μg mL^{-1} kanamycin, on an orbital shaker (100 rpm) under the continuous illumination of 20 μmol photons m^{-2} s^{-1} of warm white light, temperature of 30 °C and 2% CO_2 in the atmosphere. The inoculum cultures were replenished with fresh media every 2 weeks.

2.2. Experimental setup

2.2.1. Evaluating isoprene production in a Multi-cultivator

The strains were cultivated in a Multi-cultivator MC-1000-MIX (Photon System Instruments, PSI, Czechia) in BG-11 medium supplemented with 17 Mm HEPES buffer (pH adjusted to 8.0) and 50 μg mL^{-1} kanamycin under 50 and 100 μmol photons m^{-2} s^{-1} of violet, blue,

green and orange/red light. The illumination was provided by monochromatic LEDs with the following peaks and half-bandwidths: violet: 405 ± 20 nm, blue: 450 ± 25 nm, green: 537 ± 40 nm, red: 630 ± 25 nm (the spectra are shown in Fig. 1**a**). The cultivation was operated as a turbidostat, with the density range set to optical density measured at 720 nm (OD_{720}) of 0.52 – 0.56 (approximately 10^7 cells mL^{-1}). Temperature was maintained either at 30 °C or 35 °C. CO_2 in the bubbling gas was set to 2% (v/v) by Gas Mixing System (PSI, Czechia). The bubbling rate through each 80 mL cultivation tube was set to 60 mL min^{-1}.

After inoculation in the MC-1000-MIX, the cultures were grown for 3–5 days to reach the required turbidostat density, and then cultivated for at least 18 hours before taking samples to ensure full metabolic acclimation to the specific cultivation conditions (Zavřel et al., 2015b). Full acclimation was confirmed by the evaluation of stability of the specific growth rate, as calculated from OD_{720} and signal, and from the stability of $OD_{680\text{-}720}$ signal that reflects the concentration of chlorophyll *a* in the culture (Fig. 1**a**).

After the acclimation period, samples were withdrawn to determine parameters as described in Section 2.3. Samples were centrifuged at 4000 × *g* for 5 min and the cellular pellets were stored at −80 °C until further processing; isoprene production and photosynthetic efficiency was probed on fresh cultures using open inlet mass spectrometer and kinetic fluorometer, respectively (see Section 2.3 for details).

2.2.2. Evaluating isoprene production in the temperature range 25–45 °C

The IspS strain was cultivated in 250 mL Erlenmeyer flasks in BG-11 medium supplemented with 50 mM sodium bicarbonate, 50 Mm TES buffer (pH adjusted to 8.0) and 50 μg mL^{-1} kanamycin, under 50 μmol photons m^{-2} s^{-1} of constant white light. After an initial 3 days of cultivation, cells were centrifuged (4000 × *g*, 10 min), resuspended in fresh medium to an OD_{750} of 0.5, and 5 mL culture aliquots were transferred to 8 mL screw cap tubes (Chromacol 10-SV, Thermo Fisher Scientific). The tubes were incubated for 3–24 h at 25–45 °C with constant shaking and under 50 μmol photons m^{-2} s^{-1} of constant of white light. At the end of each cultivation, 150 μL of headspace gas was sampled for isoprene content analysis by gas chromatography (GC) (Englund et al., 2018). Growth was assessed by the measurements of culture optical density at 750 nm.

2.2.3. Testing the effect of isoprene presence on Synechocystis WT

To assess the effect of isoprene on the physiology of *Synechocystis*, the cells were first cultivated in 250 mL Erlenmeyer flasks as described in Section 2.1.3. In the active growth phase (OD_{720} < 0.3), 5 mL culture aliquots were transferred to 40 mL glass vials sealed by PTFE-coated silicone septa. Different volumes (up to 100 μL) of liquid isoprene analytical standard (≥99.5 %, Merck, Germany) were added to the headspace, in triplicates. The vials were placed into an incubator (ZWYR 240, Labwit, Australia) at either 30 or 40 °C under 30 μmol photons m^{-2} s^{-1} of constant illumination, provided by red, green and blue (RGB) custom-made LED panel (PSI, Czechia; R:G:B ratio was set to 1:1:1). After 24 h incubation, the cultures were sampled to address shifts in cell number, cell size, pigments composition and photosynthetic performance.

2.3. Analytical methods

2.3.1. Modifying MIMS for isoprene detection

In order to quantify isoprene production during the turbidostat experiments (as described in Section 2.2.1), 5 mL culture aliquots were transferred to 40 mL glass vials sealed by PTFE-coated silicone septa. The vials were placed into a tempered incubator (ZWYR 240, Labwit), previously set to correspond with the temperature of the turbidostat cultures (either 30 °C or 35 °C). To mimic the MC-1000-MIX light, the incubator was illuminated by custom-made RGB LED panel (PSI, Czechia), with LEDs matching the intensities and spectra of MC-1000-MIX light.

The isoprene content in the headspace was analyzed by modified membrane inlet mass spectrometer (MIMS; Hiden, UK) at discreet time points over a 4 h incubation. MIMS was modified by replacing the membrane inlet with an open inlet, achieved by attaching a 0.45 mm syringe needle into 1/16″ stainless steel tubing connected to a heated Quartz Inert Capillary (Hiden, UK) through 1/16″ stainless steel fitting (Swagelok, USA). Since the inlet was open, the mass spectrometer had significant sample consumption, which allowed only for discrete measurements. For further details, see Fig. 1**a** and supplementary material.

2.3.2. Pigments analysis

Content of chlorophyll *a*, total carotenoids and phycobilisomes was quantified according to the previously developed protocols (Zavřel et al., 2015a). Content of individual carotenoids was analyzed by extraction of soluble pigments in acetone and quantification by Shimadzu Prominence HPLC system (Shimadzu, Japan). HPLC was equipped with a Phenomenex Synergi Hydro-RP 250 × 4.6 mm column with a particle size of 4 μm and a pore size of 80 Å. Elution was secured by a linear gradient from solvent A (acetonitrile, water, trimethylamine:9:1:0.01) to solvent B (ethyl acetate) for 25 min at a flow rate of 1 mL min^{-1} at 25 °C.

2.3.3. Probing photosynthetic efficiency

Photosynthetic performance was probed using a Multi-Color-PAM (MC-PAM; Walz, Germany). After initial dark acclimation (10 min), OJIP curves were recorded using *FastKin_Def* trigger settings and saturation pulses of intensity 5 000 μmol photons m^{-2} s^{-1} (625 nm light). To probe the efficiency of electron transport and state transitions, Slow Kinetics MC-PAM feature was further used, with both 480 nm actinic light (AL, inducing State 1) and 625 nm AL (inducing State 2) (Calzadilla & Kirilovsky, 2020) and intensities of 80 and 50 μmol photons m^{-2} s^{-1}, respectively (both sufficiently high to induce fluorescence transients). For induction of non-photochemical quenching (NPQ), additional treatment of 480 nm AL of intensity 1 800 μmol photons m^{-2} s^{-1} was applied. Measuring light (ML) of 625 nm was used for all measurements.

2.3.4. Cell composition and morphology

Glycogen was analyzed according to the previously described protocol (Zavřel et al., 2018). Cell count and cell size were measured with Multisizer 4 COULTER COUNTER® (Beckman Coulter Inc., USA). Cellular dry weight was measured with XA105DR analytical balances (Mettler Tolledo, USA) after lyophilization of cellular pellet. The relative abundance of proteins, lipids and carbohydrates was estimated by Fourier Transformed Infrared Spectroscopy (FTIR) of lyophilized cellular pellet, using Nicolet IS10 spectrometer (Thermo Fisher Scientific) and following the previously described protocol (Felcmanová et al., 2017). Content of C, N and S in Synechocystis cells was measured by FLASH 2000 CHNS/O Analyzer (Thermo Fisher Scientific).

2.4. Flux balance analysis

Flux balance analysis (FBA) simulations were performed using the glpk solver with COBRApy version 0.24.0 (Ebrahim et al., 2013) utilizing a revised version of the previously developed FBA model (Knoop & Steuer, 2015), extended with the metabolite 'isoprene', the isoprene synthase (IspS, EC 4.2.3.27), and an isoprene demand reaction. The last step in the MEP pathway, IspH, is assumed to synthesize IPP and DMAPP in a ratio 5:1 (Adam et al., 2002).

Carbon partitioning towards isoprene was calculated as $5 \times J_{IspS} / J_{CO2,ex}$, where J_{IspS} denotes isoprene production and $J_{CO2,ex}$ denotes net uptake of CO_2 and bicarbonate HCO_3^-. Carbon partitioning towards DMAPP was calculated as $5 \times J_{DMAPP,syn} / J_{CO2,ex}$. Yields (Table 1) were estimated by minimizing total photon uptake while keeping synthesis fluxes (isoprene and biomass formation) constant. In all simulations, the

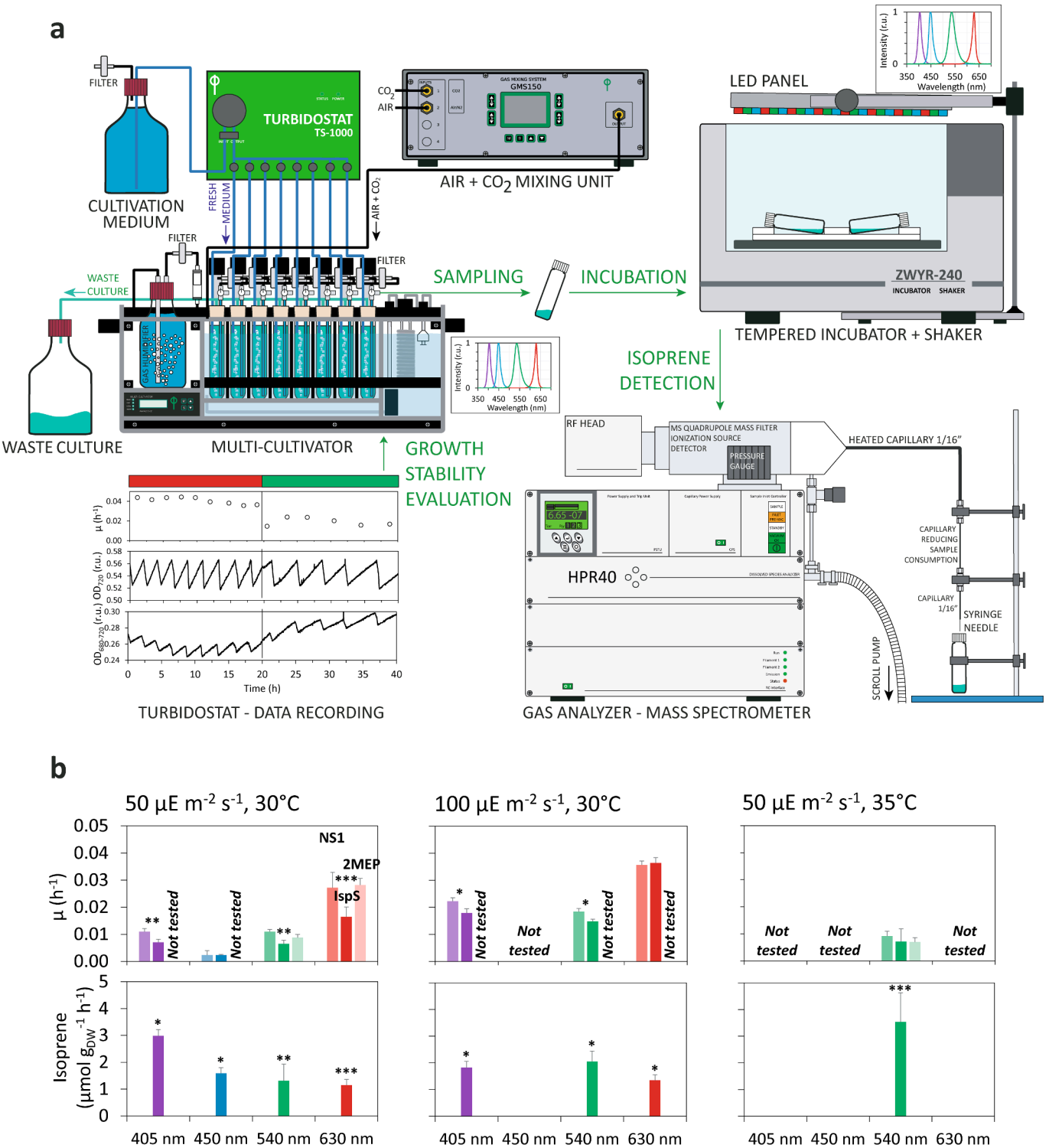

Fig. 1. Cultivation setup and culture productivity. **Panel a**: The three tested strains were cultivated in the Multi-cultivator MC-1000-MIX in a turbidostat regime. Dilution of actively growing culture by fresh cultivation medium as well as quantitative evaluation of specific growth rates was based on the measurements of optical density at 720 nm (OD_{720}). After growth stabilization under particular cultivation conditions, 5 mL culture aliquots were transferred to 40 mL vials for incubation in a tempered incubator. Light for incubations was provided by custom made LED panel and the wavelengths were identical to the MC-1000-MIX LEDs. During incubations, headspace of the gas-tight vials was sampled repeatedly over time for the evaluation of isoprene concentration. Isoprene production was evaluated by open inlet mass spectrometer. **Panel b**: Specific growth rates and isoprene productivities of NS1, 2MEP and IspS strains under the tested cultivation conditions. The values represent averages ± SD (n = 3–5). The asterisks mark parameters significantly changing between the tested strains (Kruskal-Wallis test: $p < 0.05$ (*), $p < 0.01$ (**) or $p < 0.001$ (***)).

Table 1
The upper part of the table shows a summary of different experimental conditions. For each condition, measured isoprene production and growth rate are shown, together with the calculated carbon partitioning to isoprene. From FBA simulations, CO_2 fixation and carbon partitioning to both DMAPP and to isoprene are shown. Carbon partitioning is always calculated as a percentage of total carbon in biomass and isoprene. †For the higher temperature sample, the total carbon in biomass was unusually low, resulting in a high partitioning value. The bottom part summarizes stoichiometric requirements for the synthesis of isoprene in comparison to biomass. Shown is the number of active reaction fluxes (#react), as well as the required number of photons, photons at PSII and PSI, respectively, CO_2 (all in units mmol), RuBisCO activity, and the ATP/NADPH ratio. It should be noted that RuBisCO flux slightly exceeds net CO_2 uptake due to CO_2 release in biosynthesis. ATP and NADPH requirements refer to fluxes through the ATPase and $NADP^+$ reductase. The total turnover of ATP and NADPH for the synthesis of 1 g_{DW} biomass is 209.0 mmol and 110.5 mmol, respectively. The total turnover of ATP and NADPH for the synthesis of 1 mmol isoprene is 20.0 mmol and 13.0 mmol, respectively. * ATP requirements and yield for biomass synthesis were calculated for growth on nitrate and do not include additional ATP usage for maintenance.

Cultivation setup			Measurements			Flux Balance Analysis		
Light wavelength [nm]	Light intensity [μE m^{-2} s^{-1}]	Temp. [°C]	Isoprene production rate [μmol $gDW^{-1}h^{-1}$]	Growth rate reduction [%]	C partitioning to isoprene [%]	CO_2 fixation rate [mmol $gDW^{-1}h^{-1}$]	C partitioning to DMAPP [%]	C partitioning to isoprene [%]
405	50	30	2.98	35.8	5.9	0.29	5.6	5.1
450	50	30	1.59	0.6	8.9	0.10	8.1	7.8
540	50	30	1.30	40.6	2.5	0.27	2.8	2.4
630	50	30	1.14	39.6	1.0	0.67	1.3	0.9
405	100	30	1.82	19.7	1.3	0.74	1.7	1.2
540	100	30	2.05	19.5	1.8	0.61	2.2	1.7
630	100	30	1.34	−1.9	0.5	1.45	1.0	0.5
540	50	35	3.54	21.6	11.0†	0.31	6.1	5.7

stoichiometric requirements (units: *mmol*)										
product	# react	photons	PSII	PSI	CO_2	RuBisCO	NO_3^-	ATP	NADPH	ATP/NADPH*
1 gDW biomass	512	538.3	252.6	285.7	41.5	42.0	8.8	190.5	106.1	≈ 1.80
1 g isoprene	87	822.1	411.0	411.0	73.4	88.1	0.0	249.6	190.8	≈ 1.31
1 mmol isoprene	87	56.0	28.0	28.0	5.0	6.0	0.0	17.0	13.0	≈ 1.31

ratio of photons utilized at PSII and PSI was allowed to vary freely to achieve minimal total photon uptake.

To estimate maximal isoprene synthesis and trade-offs, a constant ATP hydrolysis of $J_{NGAM} = 1.3$ mmol gDW^{-1} h^{-1} was included to account for non-growth associated maintenance (NGAM). To account for photorespiration, the carboxylation/oxidation ratio of RuBisCO was set to 97/3. For each cultivation condition, the measured glycogen content was implemented in the biomass objective function (BOF) of the model. Due to the low absolute values, the total carotenoid content was kept unchanged in the BOF. No other nutrient except photons was limiting, the only sources of carbon and nitrogen were CO_2 (taken up as bicarbonate, HCO_3^-) and nitrate (NO_3^-), respectively.

Flux maps were estimated using parsimonious FBA (pFBA), setting synthesis fluxes (isoprene and growth rate) to match the measured values and minimizing the total photon uptake. Trade-offs and the production envelopes were estimated by setting total photon flux to the value previously determined for the NS1 strain, and maximizing isoprene production for different growth rates. For computational details, see (Knoop & Steuer, 2015).

In all simulations, unless otherwise noted, photon utilization at PSII and PSI was allowed to vary freely. To test the impact of light quality (color) on growth rate for strains grown under 405 nm light, the ratio of photon utilization at PSII and PSI was constrained to fixed values. Shifting the ratio of photon utilization from the optimal $J_{PSI} / J_{PSII} = 1.3$, to $J_{PSI} / J_{PSII} = 4.3$ results in a reduction of the predicted growth rate that matched growth under 405 nm.

2.5. Statistical analysis

To identify parameters that significantly varied between the three tested strains, Kruskal-Wallis test was performed (Statistica, TIBCO, USA), by a pair-by-pair comparing of all strains. Null hypothesis was that the median of all compared groups was equal. Parameters identified as significantly changing between the strains were those that had at least one pair that differed significantly with a p-value < 0.05 ($n = 3$–5 for all strains throughout all experiments).

3. Results and discussion

3.1. Cultivation and isoprene detection

To quantify isoprene production and to assess the intracellular shifts in *Synechocystis*, the three strains IspS, 2MEP and NS1 were submitted to cultivation under distinct light qualities, light intensities and temperatures. A schematic representation of the cultivation setup is summarized in Fig. 1**a**. The strains were cultivated in MC-1000-MIX Multi-cultivator in a turbidostat regime, which allowed to reach metabolic steady-states. This was a necessary prerequisite for a comparative evaluation of all tested strains under all tested cultivation conditions (Zavřel et al., 2015b).

Given the volatile nature of isoprene (boiling point *ca.* 34 °C), the quantification of its production is best probed in closed vials. MIMS is a suitable tool for detecting volatile products in low concentrations. However, due to extremely hydrophobic nature of the isoprene molecule, routinely used silicone MIMS inlet (Zavřel et al., 2016) prevented successful isoprene pervaporation (isoprene binds to the silicone membrane so tightly that even the inner MIMS vacuum of 10^{-6} Torr is not strong enough to provide sufficient pervaporation driving force). Therefore, the only option for isoprene detection by MIMS was to sample through the modified open inlet from sealed vials and in discrete time points. The open inlet did not corrupt system sensitivity or linearity (see supplementary material for details).

3.2. Effect of light quality on isoprene production

Isoprene production was quantified under monochromatic violet, blue, green and red lights, to match absorption peaks of chlorophyll *a* (blue light) and phycobilisomes (red light) as well as to test additional wavelengths favourable for the growth of phycocyanin-containing cyanobacteria (violet, green (Bernát et al., 2021)). Growth rate of all strains was dependent on the wavelength of the incident light. Growth was the slowest under blue light, increased under green and violet light, and the fastest under red light (Fig. 1**b**), reflecting wavelength-specific alterations related to shifts in the redox state of the PQ pool, ATP:NADPH or PSII:PSI ratio (Bernát et al., 2021; Singh et al., 2009). Growth rate of the isoprene producer IspS was reduced compared to the NS1 control strain

under all tested lights but blue (Fig. 1**b**, Table 1), which suggests a reallocation of ATP, NADPH and reduced ferredoxin (Fd^{red}) from pathways related to growth (cell division, biomass formation) to pathways related to isoprene production. This is in line with only a slight reduction of growth rate in strain 2MEP compared to the NS1 control, as tested under green and red light (Fig. 1**b**). The situation was different for blue light, which is preferentially absorbed by PSI rather than by PSII (Singh et al., 2009). Providing only blue light to *Synechocystis* causes severe metabolic and redox imbalance, which results in reduced linear electron flow and increased cyclic electron flow around PSI, and leads to an increased ATP:NADPH ratio (Singh et al., 2009). As a result, carbon fixation and growth rate are reduced, mainly due to the lack of reducing equivalents (Bernát et al., 2021; Singh et al., 2009).

Isoprene production in the IspS strain had similar rates under red, green and blue light (Fig. 1**b**). Only the violet light allowed for increased isoprene production, indicating an increased carbon redirecting towards isoprene biosynthesis (Table 1). Higher carbon partitioning towards the MEP pathway was also reflected by increased synthesis of carotenoids (myxoxanthophyll, zeaxanthin) in the IspS strain under violet light (see supplementary material for details).

Regardless of the monochromatic light used, the IspS strain showed reduced content of phycobilisomes and chlorophyll *a* (Fig. 2**b**) compared to the control strains. Carotenoids, on the other hand, were generally upregulated in IspS and 2MEP strains, that both overexpress DXS and IDI (Fig. 2**b**). Since DXS catalyses the irreversible conversion of pyruvate and glyceraldehyde 3-phosphate (G3P) into deoxy-*D*-xylulose 5-phosphate (DXP), its overexpression was hypothesized to reallocate more carbon to the MEP pathway. The increased carotenoid content confirmed such reallocation. Further addition of a non-native terpene synthase then channelled part of the flux towards the synthesis of isoprene.

Cyanobacterial carotenoids include mainly β-carotene, zeaxanthin, echinenone and its 3′-hydroxylated form, synechoxanthin and myxol glycosides (also known as myxoxanthophylls), each presenting slightly different roles in the physiology of the cell (Takaichi & Mochimaru, 2007). β-carotene was decreased in the IspS strain but increased in the 2MEP strain compared to the NS1 control. Xantophylls, on the other hand, were generally upregulated in both IspS and 2MEP strains (see supplementary material for details). As further discussed in Section 3.6, increased consumption of β-carotene for xantophylls biosynthesis in the IspS strain can potentially be attributed to the presence of isoprene itself and to alterations of its thylakoid membranes (see supplementary material for details). Similarly, the reduced cell size and higher non-photochemical quenching in the IspS strain (NPQ, Fig. 2) are likely a result of the isoprene presence in the cells (Fig. 3**c**).

The reduction of growth rate of the IspS strain can be partially attributed to the decline of the linear electron transport rate (ETR), which was likely linked to downregulation of light harvesting antenna as well as to the reduced ability to fine-tune light harvesting through state transitions (Fig. 2**c**). The production of isoprene did not have any effect on total cellular protein pool, but it induced alterations in the content of glycogen and partially of lipids (Fig. 2**a;** for further details see supplementary material).

In line with previous works (Bernát et al., 2021) PQ pool was in general reduced under violet and blue light. Under green and red light (lower PQH_2/PQ), overexpression of the MEP pathway influenced cellular redox state, as the PQ pool became substantially more reduced in both IspS and 2MEP strains compared to the control strain NS1 (see supplementary material for details).

3.3. *Effect of light intensity on isoprene production*

Further, the effect of increased light intensity on isoprene production was tested. The IspS and NS1 strains were cultivated under 100 μmol photons m^{-2} s^{-1} of red, green and violet light (referred as high light hereafter), following the same culture acclimation and sampling

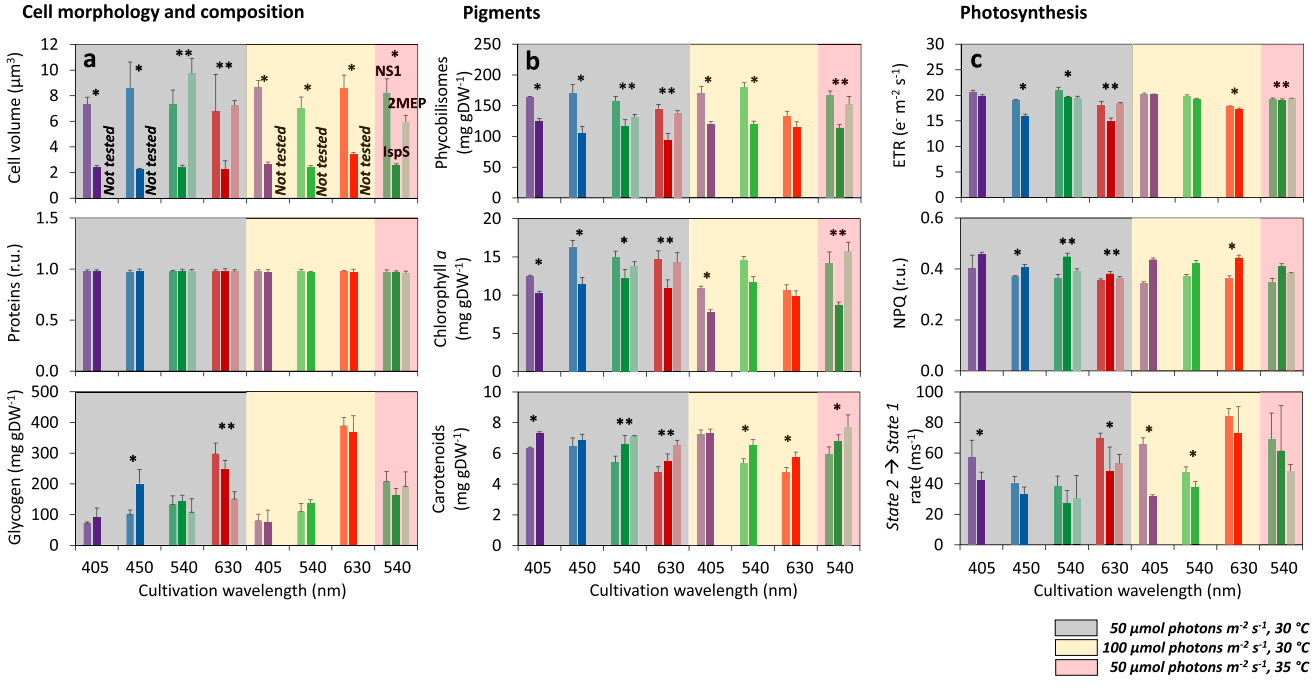

Fig. 2. Effect of light quality, light intensity and temperature on cell volume, cell composition and photosynthetic performance of NS1 (left bars), 2MEP (middle bars) and IspS (right bars) strains. Under low light intensity (grey), increased light intensity (yellow) and increased temperature (pink), the following parameters were estimated: cellular volume, protein and glycogen content (a), pigment composition (b), electron transport rate, non-photochemical quenching and state transition rates (c). The values represent averages ± SD (n = 3–5). The asterisks mark parameters significantly changing between the tested strains (Kruskal-Wallis test: $p < 0.05$ (*), $p < 0.01$ (**)).

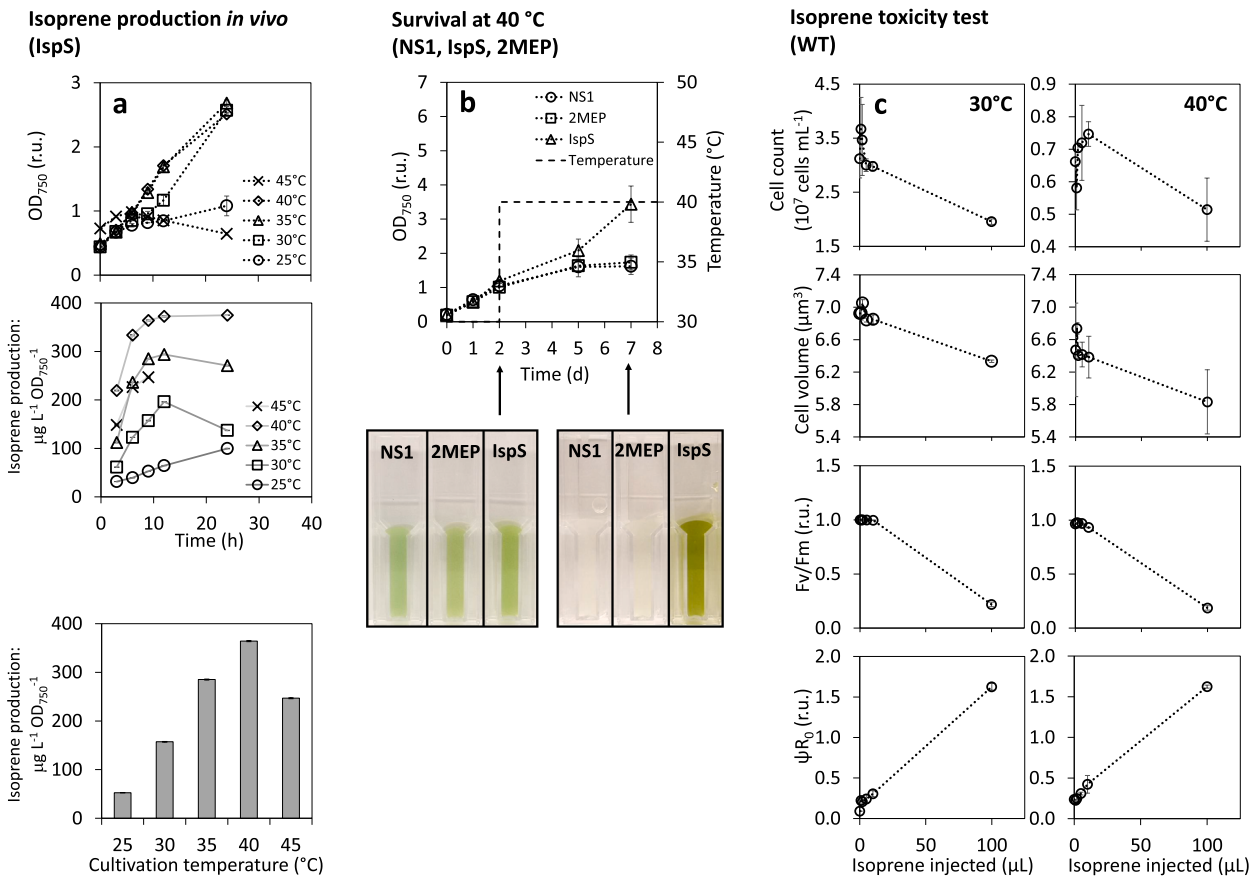

Fig. 3. Temperature characterization of *in vivo* isoprene production by the IspS strain in temperature range 25–45 °C (**a**), response to the increased temperature (30 °C → 40 °C) of the strains NS1, 2MEP and IspS (**b**) and the effect of externally added isoprene on the physiology of *Synechocystis* sp. PCC 6803 WT (**c**). The *in vivo* temperature characterization of isoprene production (panel **a**, bottom) was evaluated after 9 h of cultivation (panel **a**, top), however, the isoprene production was followed for 24 h for most conditions (panel **a**, middle). All cultivations were performed in glass vials sealed by PTFE-coated silicon/rubber septa, the values represent averages ± SD (n = 3–5). The isoprene injected (panel **c**) represents amount externally added isoprene liquid standard to 40 mL vials that contained 5 mL culture aliquots.

procedures as described in sections 2.2.1 and 3.1. Blue light was not considered for high light treatment since it was the least favourable for *Synechocystis* growth and did not provide a positive effect on isoprene production. Both IspS and NS1 strains had an increased specific growth rate under all tested high light conditions (Fig. 1**b**). However, the isoprene production increased only slightly under high green and red lights, whereas under high violet light the isoprene production even decreased (Fig. 1**b**). This suggests that isoprene synthesis is not directly coupled to cellular growth, in agreement with the results of growth and isoprene production under blue light as measured here (Fig. 1**b**), as well as with the earlier report on higher isoprene production in later stages of batch growth (Gao et al., 2016). As recently shown for another product of metabolism (lactate), separation of growth and production phases can be a strategy to achieve high yields (Shabestary et al., 2021).

Trends in cell volume, cell composition and photosynthesis performance of the IspS strain in comparison with NS1 control followed trends observed under 50 µmol photons m^{-2} s^{-1}. (Fig. 2**,** for further details see supplementary material). Considering the reduced efficiency of carbon and light partitioning into isoprene (Table 1) under 100 µmol photons m^{-2} s^{-1}, no further tests under increasing light intensities were performed, and the effect of increased temperature on isoprene production was explored instead.

3.4. Effect of increased temperature on isoprene production

The temperature optimum for *Synechocystis* turbidostatic growth was previously identified to be around 35 °C. However, it was also identified as shifting between individual *Synechocystis* substrains (Zavřel et al., 2017). The identical growth rates at both 30 °C and 35 °C of all strains under green light as found here (Fig. 1**b**; Kruskal-Wallis: p greater than 0.05) are in line with previously reported temperature optimum of *Synechocystis* substrain PCC-B (Zavřel et al., 2017). Trends in cell volume, cell composition and photosynthesis performance of all tested strains were also similar at 35 °C, compared to 30 °C (Fig. 2).

Most isoprene synthases are known to work efficiently at higher temperatures (up to 50 °C) (Monson et al., 1992). Therefore, the isoprene production in turbidostat at the optimal growth temperatures of 30 °C and 35 °C was tested (Fig. 1**b**), and the isoprene production in batch cultures was further evaluated in the temperature range of 25–45 °C (Fig. 3**a**). The turbidostat experiments were performed under green light, in order to balance cell growth and isoprene production.

Trends in cell volume, cell composition and photosynthesis performance of all tested strains were similar at 35 °C, compared to 30 °C (Fig. 2). The most significant change at 35 °C was in isoprene production by the IspS strain: raising the temperature by 5 °C resulted in a two-fold increase in isoprene production (Fig. 1**b**). Although temperature dependency of the particular isoprene synthase used in this study was not tested, it is likely that the temperature increase was beneficial for its catalytic activity (Monson et al., 1992). Additionally, considering that the boiling point of isoprene is *ca.* 34 °C, cultivation of the engineered cells at 35 °C favored isoprene accumulation in gaseous headspace of the closed vials.

To understand the overall effect of temperature on the isoprene production, a series of 24 h incubations in the temperature range 25–45 °C was performed, and *in vivo* temperature optimum of isoprene production was identified at 40 °C (Fig. 3**a**). It should be noted that since the biochemical characterization of the enzyme was not performed, contribution of individual factors to the increased isoprene production at elevated temperature remains to be elucidated. These factors include catalytic efficiency of the terpene synthase, and/or changes in the metabolism and/or altered physiology of *Synechocystis* cells, including higher membrane fluidity (Velikova et al., 2011).

3.5. Effect of isoprene presence on thermotolerance in Synechocystis

The IspS strain was able to grow well even at 40 °C (Fig. 3**b**). This significantly extends the range for *Synechocystis* cultivation; previous works report maximum growth temperature of *Synechocystis* to be 38 °C (Zavřel et al., 2017). To confirm the positive effect of isoprene on thermotolerance, the three strains were cultivated in open Erlenmeyer flasks first at 30 °C for two days, and then at 40 °C for five days. While both NS1 and 2MEP control strains were not able to survive the prolonged exposure to 40 °C, the isoprene producer grew well at 40 °C and its cultures retained a healthy green colour even after five days of cultivation at 40 °C (Fig. 3**b**).

In plants, isoprene is produced as a defence mechanism against heat stress. Despite gaps in knowledge of its true action mechanism (Pollastri et al., 2021; Zuo et al., 2019), the current consensus assumes isoprene role in thylakoid membranes stabilization (Velikova et al., 2011). The increased heat tolerance of the IspS strain as reported here not only strengthens the previous findings on the isoprene role in adaptation to elevated temperature, but also demonstrates that such response mechanism can be transferred to other organisms via heterologous expression of the isoprene synthase. This finding opens the possibility of using isoprene-producing cyanobacteria to studying thermotolerance mechanisms in a plant-like model system, and leads to a new perspective for thermotolerance improvement in biotechnologically relevant strains.

3.6. Effects of isoprene on Synechocystis cell physiology

Under all tested conditions, the IspS cells were 2 to 3 times smaller in volume than the control strains (Fig. 2). Hydrocarbons have been demonstrated to concentrate in thylakoid membranes and alter membranes morphology (Lea-Smith et al., 2016). To investigate the effect of the isoprene presence on *Synechocystis* morphology in detail, a series of additional experiments was conducted. The cultures of *Synechocystis* WT strain were cultivated in closed vials at 30 °C and 40 °C in the presence of externally injected isoprene standard for 24 h. As expected, the presence of isoprene led to a reduction of cell volume (Fig. 3**c**). In general, the highest isoprene addition of 100 μL (to 5 mL of culture aliquots in 40 mL vials) was toxic for *Synechocystis* cells, as it resulted in very poor performance of all cultures. However, lower isoprene concentrations (≤10 μL injected) allowed *Synechocystis* to increase the cell number at 40 °C (Fig. 3**c**), whereas at 30 °C, an identical amount of injected isoprene led to a cell number reduction. This finding again demonstrated the positive effect of isoprene towards thermo-tolerance improvement, even when added extracellularly to *Synechocystis* WT cells.

Considering the hydrophobic nature of isoprene and previous reports on hydrocarbons accumulation in thylakoid membranes (Monson et al., 1992; Lea-Smith et al., 2016), it is likely that this small terpene is accumulating in the lipid bilayers and affects fluidity of the lipid membranes. Such membrane alterations would also explain changes in photosynthetic parameter ψR_0 (Fig. 3**c**) and distribution of carotenoids (see supplementary material for details), in addition to shifts in cell size and specific growth rate. The parameter ψR_0 describes the efficiency with which a PSII-trapped electron is transferred to the final PSI acceptors (Stirbet et al., 2018). With increased membrane fluidity, ψR_0 can be expected to increase. Since a linear correlation between ψR_0 and isoprene amount injected into the *Synechocystis* culture was found, it is likely that the dependency of the membrane fluidity on isoprene concentration is also linear.

The increased membrane fluidity was likely a driving force responsible for favouring xanthophylls and partially also myxoxanthophyll synthesis over β-carotene in the IspS strain as well as in the WT strain after isoprene addition (see supplementary material for details). Since β-carotene can be found both in photocenters (PSI, PSII) and in membranes, and xanthophylls and myxoxantophyll are present exclusively in thylakoid membranes where they maintain their stability (Mohamed et al., 2005; Zakar et al., 2017), it is likely that the increase in xanthophylls and myxoxantophyll biosynthesis was triggered by the increase in membrane fluidity due to the presence of isoprene. These results further demonstrate complex isoprene interactions in *Synechocystis* cells.

3.7. FBA and modelling of isoprene production

The results for isoprene production were further evaluated in the context of a genome-scale metabolic model of *Synechocystis* metabolism (Knoop & Steuer, 2015; Knoop et al., 2013). Based on a comprehensive stoichiometric reconstruction of *Synechocystis* metabolism, the model allowed to evaluate maximal yields, growth rates, and carbon partitioning in the NS1 control and engineered IspS strains. To this end, a model of the WT strain of *Synechocystis* (corresponding to the NS1 strain) was augmented by the IspS reaction for isoprene synthesis.

The stoichiometric model gives rise to a maximal yield per photon for biomass $Y_{photon}^{BM} \approx 1.86\ g_{DW}\ mol_{photons}^{-1}$, and a yield of isoprene per photon $Y_{photon}^{gisp} \approx 1.22\ g_{isoprene}\ mol_{photons}^{-1}$. Further stoichiometry properties are summarized in Table 1.

Specifically, synthesis of 1 mol of isoprene requires 56 mol of photons (absorbed equally at PSII and PSI), a supply of 17 mol of ATP by the ATPase, and a supply of 13 mol of NADPH by the $NADP^+$ reductase. The ATP and redox requirements for isoprene match linear electron transport. The total turnover of ATP per mol of isoprene is slightly higher (20 mol) since the MEP pathway generates two pyrophosphates, and one ATP is generated by the pyruvate kinase. The ratio of ATP:NADPH demand for isoprene synthesis (ATP:NADPH ≈ 1.31) is lower than the ratio ATP:NADPH ≈ 1.8 required for biomass synthesis. The reduced demand for ATP compared to biomass synthesis is characteristic for most products, and likely results in a surplus of ATP in production strains (Knoop & Steuer, 2015).

The genome-scale model further allows to computationally estimate intracellular fluxes that correspond to the observed rate of growth and isoprene synthesis. Fig. 4**a** shows the predicted metabolic flux map for NS1 and IspS strains for a light intensity of 100 μmol photons $m^{-2}\ s^{-1}$ red (630 nm) light. Flux predictions are obtained by computational optimization and can be interpreted as lower bounds on the required fluxes that are consistent with the measured output flux.

Synthesis of isoprene incurs a cost on growth. The predicted trade-off can be estimated using a production envelope, shown in Fig. 4**b-c**. The curves show the (hypothetical) maximal stoichiometric rates of isoprene synthesis given the measured growth rate of the NS1 strain, together with the experimentally achieved rates. The production envelopes indicate that stoichiometric partitioning of carbon precursors is not sufficient to explain the observed reduction in growth rate. The results are further detailed in Table 1. Given the estimated carbon partitioning, it is not expected that imbalances in co-factor requirements (in particular ATP and NADPH) can explain the reduced growth rates. This is in line with the previous observation that isoprene production is not directly coupled to growth and the limitations in isoprene synthesis are not due to competition for carbon precursors or co-factors.

4. Conclusions

In this study, the isoprene production in *Synechocystis* was quantified

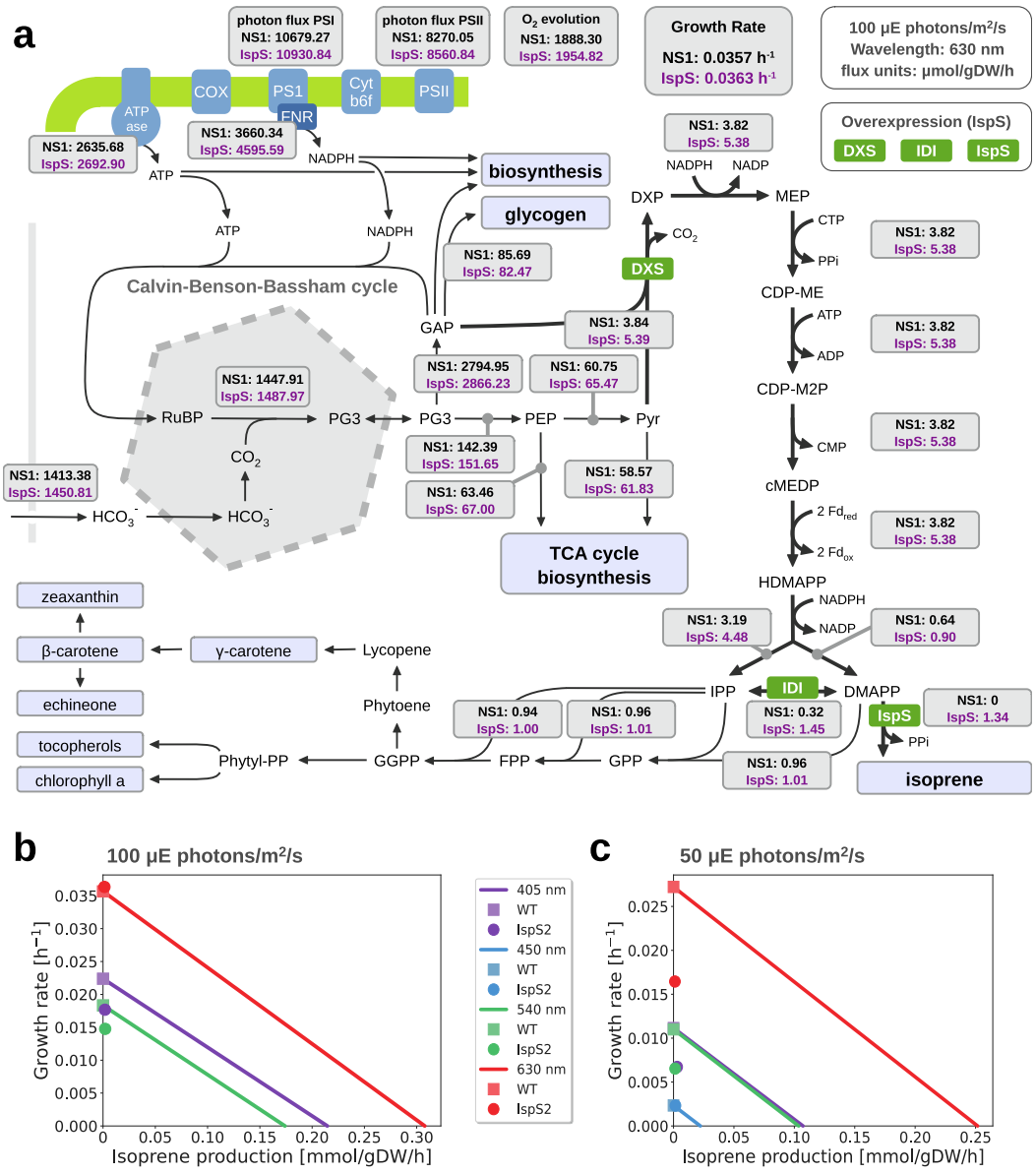

Fig. 4. Predicted metabolic flux map for 100 µmol photons m^{-2} s^{-1} red (630 nm) light (**a**). Flux predictions were obtained by minimizing the photon uptake rate given the measured rates of isoprene production and growth for the NS1 and IspS strain. Hence, flux predictions can be interpreted as lower bounds on the required fluxes that are consistent with measured synthesis flux. (b) Production envelope for 100 µmol photons m^{-2} s^{-1}, 30 °C. Shown are the (hypothetical) maximal isoprene productions given the measured growth rates (lines), as well as the observed values for different light intensities. (c) Production envelope for 50 µmol photons m^{-2} s^{-1}, 30 °C. (For interpretation of the references to color in this figure legend, the reader is referred to the web version of this article.)

by modified MIMS under a range of light qualities, light intensities and temperatures and further analysed by flux balance analysis in order to obtain full distribution of metabolic fluxes. The effect of the physical presence of isoprene on *Synechocystis* physiology and morphology was evaluated. It was demonstrated that isoprene presence improves thermotolerance in cyanobacteria, and that this improvement can be transferred between organisms. The comprehensive approach and results are expected to lead the way towards biotechnologically feasible production of isoprene and other terpenes.

E-supplementary data for this work can be found in e-version of this paper online.

CRediT authorship contribution statement

João S. Rodrigues: Conceptualization, Data curation, Formal analysis, Investigation, Methodology, Writing – original draft, Writing – review & editing. **László Kovács:** Methodology, Data curation, Writing – review & editing. **Martin Lukeš:** Methodology, Data curation, Writing – review & editing. **Rune Höper:** Methodology, Software, Writing – review & editing. **Ralf Steuer:** Methodology, Software, Supervision, Writing – review & editing. **Jan Červený:** Funding acquisition, Resources, Writing – review & editing. **Pia Lindberg:** Funding acquisition, Resources, Supervision, Visualization, Writing – review & editing. **Tomáš Zavřel:** Conceptualization, Data curation, Formal analysis, Investigation, Methodology, Project administration, Supervision, Validation, Visualization, Writing – original draft, Writing – review & editing.

Declaration of Competing Interest

The authors declare that they have no known competing financial interests or personal relationships that could have appeared to influence

the work reported in this paper.

Data availability

Data will be made available on request.

Acknowledgements

This work was supported by the Swedish Energy Agency (project number 38334–3), by the NordForsk NCoE program "NordAqua" (project number 82845), by the Ministry of Education, Youth and Sports of CR (OP RDE, grant number CZ.02.1.01/0.0/0.0/16_026/0008413 'Strategic Partnership for Environmental Technologies and Energy Production'), and it is based on use of Large Research Infrastructure CzeCOS supported within the CzeCOS program (grant number LM2023048). RH and RS were supported by the DFG grant 453048493. Special thanks belong to Tomáš Zlámal for technical assistance with MIMS modifications.

Appendix A. Supplementary data

Supplementary data to this article can be found online at https://doi.org/10.1016/j.biortech.2023.129068.

References

Adam, P., Hecht, S., Eisenreich, W., Kaiser, J., Grawert, T., Arigoni, D., Bacher, A., Rohdich, F., 2002. Biosynthesis of terpenes: studies on 1-hydroxy-2-methyl-2-(E)-butenyl 4-diphosphate reductase. PNAS 99 (19), 12108–12113.

Banerjee, A., Sharkey, T.D., 2014. Methylerythritol 4-phosphate (MEP) pathway metabolic regulation. Nat. Prod. Rep. 31 (8), 1043–1055.

Bernát, G., Zavřel, T., Kotabová, E., Kovács, L., Steinbach, G., Vörös, L., Prášil, O., Somogyi, B., Tóth, V.R., 2021. Photomorphogenesis in the Picocyanobacterium *Cyanobium gracile* Includes Increased Phycobilisome Abundance Under Blue Light, Phycobilisome Decoupling Under Near Far-Red Light, and Wavelength-Specific Photoprotective Strategies. *Frontiers*. Plant Sci. 12.

Calzadilla, P.I., Kirilovsky, D., 2020. Revisiting cyanobacterial state transitions. Photochem. Photobiol. Sci. 19 (5), 585–603.

Chaves, J.E., Melis, A., 2018. Engineering isoprene synthesis in cyanobacteria. FEBS Lett. 592 (12), 2059–2069.

Ebrahim, A., Lerman, J.A., Palsson, B.O., Hyduke, D.R., 2013. COBRApy: COnstraints-Based Reconstruction and Analysis for Python. BMC Syst. Biol. 7, 74.

Englund, E., Shabestary, K., Hudson, E.P., Lindberg, P., 2018. Systematic overexpression study to find target enzymes enhancing production of terpenes in *Synechocystis* PCC 6803, using isoprene as a model compound. Metab. Eng. 49, 164–177.

Felcmanová, K., Lukeš, M., Kotabová, E., Lawrenz, E., Halsey, K.H., Prášil, O. 2017. Carbon use efficiencies and allocation strategies in *Prochlorococcus marinus* strain PCC 9511 during nitrogen-limited growth. *Photosynthesis Research*, **134**(1), 71-82.

Gao, X., Gao, F., Liu, D., Zhang, H., Nie, X., Yang, C., 2016. Engineering the methylerythritol phosphate pathway in cyanobacteria for photosynthetic isoprene production from CO_2. Energ. Environ. Sci. 9 (4), 1400–1411.

Guenther, A., Hewitt, C.N., Erickson, D., Fall, R., Geron, C., Graedel, T., Harley, P., Klinger, L., Lerdau, M., Mckay, W.A., Pierce, T., Scholes, B., Steinbrecher, R., Tallamraju, R., Taylor, J., Zimmerman, P., 1995. A global model of natural volatile organic compound emissions. J. Geophys. Res. Atmos. 100 (D5), 8873–8892.

Heidorn, T., Camsund, D., Huang, H.H., Lindberg, P., Oliveira, P., Stensjö, K., Lindblad, P., 2011. Synthetic biology in cyanobacteria: Engineering and analyzing novel functions. Methods Enzymol. 497, 539–579.

Klaus, O., Hilgers, F., Nakielski, A., Hasenklever, D., Jaeger, K.-E., Axmann, I.M., Drepper, T., 2022. Engineering phototrophic bacteria for the production of terpenoids. Curr. Opin. Biotechnol. 77, 102764.

Knoop, H., Steuer, R., 2015. A computational analysis of stoichiometric constraints and trade-offs in cyanobacterial biofuel production. Front. Bioeng. Biotechnol. 3, 47.

Knoop, H., Grundel, M., Zilliges, Y., Lehmann, R., Hoffmann, S., Lockau, W., Steuer, R., 2013. Flux balance analysis of cyanobacterial metabolism: the metabolic network of *Synechocystis* sp. PCC 6803. PLoS Comput. Biol. 9 (6), e1003081.

Kunert, A., Hagemann, M., Erdmann, N., 2000. Construction of promoter probe vectors for *Synechocystis* sp. PCC 6803 using the light-emitting reporter systems Gfp and LuxAB. J. Microbiol. Methods 41 (3), 185–194.

Kuzma, J., Nemecek-Marshall, M., Pollock, W.H., Fall, R., 1995. Bacteria produce the volatile hydrocarbon isoprene. Curr. Microbiol. 30 (2), 97–103.

Lea-Smith, D.J., Ortiz-Suarez, M.L., Lenn, T., Nürnberg, D.J., Baers, L.L., Davey, M.P., Parolini, L., Huber, R.G., Cotton, C.A.R., Mastroianni, G., Bombelli, P., Ungerer, P., Stevens, T.J., Smith, A.G., Bond, P.J., Mullineaux, C.W., Howe, C.J., 2016. Hydrocarbons Are Essential for Optimal Cell Size, Division, and Growth of Cyanobacteria. Plant Physiol. 172 (3), 1928–1940.

Lindberg, P., Park, S., Melis, A., 2010. Engineering a platform for photosynthetic isoprene production in cyanobacteria, using *Synechocystis* as the model organism. Metab. Eng. 12 (1), 70–79.

Mohamed, H.E., van de Meene, A.M.L., Robertson, R.W., Vermaas, W.F.J., 2005. Myxoxanthophyll Is Required for Normal Cell Wall Structure and Thylakoid Organization in the Cyanobacterium *Synechocystis* sp. Strain PCC 6803. Journal of Bacteriology 187 (20), 6883–6892.

Monson, R.K., Jaeger, C.H., Adams, W.W., Driggers, E.M., Silver, G.M., Fall, R., 1992. Relationships among Isoprene Emission Rate, Photosynthesis, and Isoprene Synthase Activity as Influenced by Temperature. Plant Physiol. 98 (3), 1175–1180.

Nirati, Y., Purushotham, N., Alagesan, S., 2022. Quantitative insight into the metabolism of isoprene-producing *Synechocystis* sp. PCC 6803 using steady state 13C-MFA. Photosynth. Res. 154 (2), 195–206.

Pollastri, S., Baccelli, I., Loreto, F., 2021. Isoprene: An Antioxidant Itself or a Molecule with Multiple Regulatory Functions in Plants? Antioxidants 10 (5), 684.

Rana, A., Cid Gomes, L., Rodrigues, J.S., Yacout, D.M.M., Arrou-Vignod, H., Sjölander, J., Proos Vedin, N., El Bakouri, O., Stensjö, K., Lindblad, P., Andersson, L., Sundberg, C., Berglund, M., Lindberg, P., Ottosson, H., 2022. A combined photobiological–photochemical route to C10 cycloalkane jet fuels from carbon dioxide via isoprene. Green Chem. 24 (24), 9602–9619.

Rodrigues, J.S., Lindberg, P., 2021. Engineering Cyanobacteria as Host Organisms for Production of Terpenes and Terpenoids. Cyanobacteria Biotechnology 267–300.

Rohmer, M., 1999. The discovery of a mevalonate-independent pathway for isoprenoid biosynthesis in bacteria, algae and higher plants. Nat. Prod. Rep. 16 (5), 565–574.

Shabestary, K., Hernández, H.P., Miao, R., Ljungqvist, E., Hallman, O., Sporre, E., Branco dos Santos, F., Hudson, E.P., 2021. Cycling between growth and production phases increases cyanobacteria bioproduction of lactate. Metab. Eng. 68, 131–141.

Sharkey, T.D., Yeh, S., 2001. Isoprene Emission From Plants. Annu. Rev. Plant. Physiol. Plant. Mol. Biol. 52 (1), 407–436.

Singh, A.K., Bhattacharyya-Pakrasi, M., Elvitigala, T., Ghosh, B., Aurora, R., Pakrasi, H. B., 2009. A Systems-Level Analysis of the Effects of Light Quality on the Metabolism of a Cyanobacterium *Plant Physiology* 151 (3), 1596–1608.

Singsaas, E.L., Lerdau, M., Winter, K., Sharkey, T.D., 1997. Isoprene Increases Thermotolerance of Isoprene-Emitting Species. Plant Physiol. 115 (4), 1413–1420.

Stanier, R.Y., Kunisawa, R., Mandel, M., Cohen-Bazire, G., 1971. Purification and properties of unicellular blue-green algae (order *Chroococcales*). Bacteriol. Rev. 35 (2), 171–205.

Stirbet, A., Lazár, D., Kromdijk, J., Govindjee., 2018. Chlorophyll a fluorescence induction: Can just a one-second measurement be used to quantify abiotic stress responses? Photosynthetica 56 (1), 86–104.

Takaichi, S., Mochimaru, M., 2007. Carotenoids and carotenogenesis in cyanobacteria: unique ketocarotenoids and carotenoid glycosides. Cell. Mol. Life Sci. 64 (19–20), 2607–2619.

Velikova, V., Várkonyi, Z., Szabó, M., Maslenkova, L., Nogues, I., Kovács, L., Peeva, V., Busheva, M., Garab, G., Sharkey, T.D., Loreto, F., 2011. Increased Thermostability of Thylakoid Membranes in Isoprene-Emitting Leaves Probed with Three Biophysical Techniques. Plant Physiol. 157 (2), 905–916.

Wagner, W.P., Helmig, D., Fall, R., 2000. Isoprene biosynthesis in *Bacillus subtilis* via the methylerythritol phosphate pathway. J. Nat. Prod. 63 (1), 37–40.

Whited, G.M., 2010. TECHNOLOGY UPDATE: Development of a gas-phase bioprocess for isoprene-monomer production using metabolic pathway engineering. Ind. Biotechnol. 6 (3), 152–163.

Zakar, T., Herman, E., Vajravel, S., Kovacs, L., Knoppová, J., Komenda, J., Domonkos, I., Kis, M., Gombos, Z., Laczko-Dobos, H., 2017. Lipid and carotenoid cooperation-driven adaptation to light and temperature stress in *Synechocystis* sp. PCC6803. *Biochimica et Biophysica Acta (BBA)* -. Bioenergetics 1858 (5), 337–350.

Zavřel, T., Sinetova, M.A., Červený, J., 2015a. Measurement of Chlorophyll *a* and Carotenoids Concentration in Cyanobacteria. Bio-protocol 5 (9), e1467.

Zavřel, T., Sinetova, M.A., Búzová, D., Literáková, P., Červený, J., 2015b. Characterization of a model cyanobacterium *Synechocystis* sp. PCC 6803 autotrophic growth in a flat-panel photobioreactor. Eng. Life Sci. 15 (1), 122–132.

Zavřel, T., Knoop, H., Steuer, R., Jones, P.R., Červený, J., Trtílek, M., 2016. A quantitative evaluation of ethylene production in the recombinant cyanobacterium *Synechocystis* sp. PCC 6803 harboring the ethylene-forming enzyme by membrane inlet mass spectrometry. Bioresour. Technol. 202, 142–151.

Zavřel, T., Očenášová, P., Červený, J., 2017. Phenotypic characterization of *Synechocystis* sp. PCC 6803 substrains reveals differences in sensitivity to abiotic stress. PLoS One 12, e0189130.

Zavřel, T., Očenášová, P., Sinetova, M.A., Červený, J., 2018. Determination of Storage (Starch/Glycogen) and Total Saccharides Content in Algae and Cyanobacteria by a Phenol-Sulfuric Acid Method. Bio Protoc 8 (15), e2966.

Zuo, Z., Weraduwage, S.M., Lantz, A.T., Sanchez, L.M., Weise, S.E., Wang, J., Childs, K. L., Sharkey, T.D., 2019. Isoprene Acts as a Signaling Molecule in Gene Networks Important for Stress Responses and Plant Growth. Plant Physiol. 180 (1), 124–152.